CANCER

Anti–PD-1 antitumor immunity is enhanced by local and abrogated by systemic chemotherapy in GBM

Dimitrios Mathios,[1]* Jennifer E. Kim,[1]* Antonella Mangraviti,[1] Jillian Phallen,[1,2] Chul-Kee Park,[1,3] Christopher M. Jackson,[1] Tomas Garzon-Muvdi,[1] Eileen Kim,[1] Debebe Theodros,[1] Magdalena Polanczyk,[4] Allison M. Martin,[2] Ian Suk,[1] Xiaobu Ye,[1] Betty Tyler,[1] Chetan Bettegowda,[1] Henry Brem,[1] Drew M. Pardoll,[4] Michael Lim[1]†

The immunosuppressive effects of chemotherapy present a challenge for designing effective cancer immunotherapy strategies. We hypothesized that although systemic chemotherapy (SC) exhibits negative immunologic effects, local chemotherapy (LC) can potentiate an antitumor immune response. We show that LC combined with anti–programmed cell death protein 1 (PD-1) facilitates an antitumor immune response and improves survival ($P < 0.001$) in glioblastoma. LC-treated mice had increased infiltration of tumor-associated dendritic cells and clonal expansion of antigen-specific T effector cells. In comparison, SC resulted in systemic and intratumoral lymphodepletion, with decreased immune memory in long-term survivors. Furthermore, adoptive transfer of CD8^{+} cells from LC-treated mice partially rescued SC-treated mice after tumor rechallenge. Last, the timing of chemo- and immunotherapy had differential effects on anti–PD-1 efficacy. This study suggests that both mode of delivery and timing have distinct effects on the efficacy of anti–PD-1. The results of this work could help guide the selection and scheduling of combination treatment for patients with glioblastoma and other tumor types.

INTRODUCTION

Glioblastoma (GBM) is the most common and aggressive primary brain tumor in adults, with an expected survival of less than 2 years despite multimodal interventions (1). Although GBM rarely metastasizes, these tumors and their treatment have systemic sequelae, including severe immunosuppression (2, 3). Current standard of care includes surgery, systemic temozolomide (TMZ), and radiation. Systemic chemotherapy (SC) is thought to damage the bone marrow (BM) and subsequently affect the number and activation state of resident immune cells (4), raising concerns for potential antagonistic interactions between SC and immunotherapy.

Anti–programmed cell death protein 1 (PD-1) monoclonal antibodies (mAbs) have emerged as a promising therapeutic strategy against a number of solid tumors (5, 6). These mAbs target PD-1, a receptor expressed on the membrane of tumor-infiltrating lymphocytes (TILs) that, once activated, results in decreased survival and proliferation of CD8^{+} T cells, reduced cytokine production, and T cell exhaustion. Blocking the interaction between PD-1 and its ligands (PD-L1 and PD-L2) restores T cell function to promote an antitumor immune response (7). However, effective implementation of immunotherapy alongside conventional cancer therapies requires careful study of the potential synergistic or antagonistic effects of concomitant modalities. The potential for the lymphodepleting effects of chemotherapy to blunt the activity of immunotherapeutic agents is of particular concern (8, 9).

We hypothesized that local chemotherapy (LC)—unlike SC—mitigates chemotherapy-associated immunosuppression and potentiates an antitumor immune response (9). The preclinical studies described here compare the effects of SC and LC on anti–PD-1 efficacy

and give insight into the effect of timing chemotherapy in relation to immunotherapy.

RESULTS

SC is immunosuppressive

For the experiments currently presented in the manuscript, we used the following schedules: Carmustine [bis-chloroethylnitrosurea (BCNU)] was given by intraperitoneal injection at varying doses (5, 15, and 30 mg/kg) after anti–PD-1 treatment. A dose of 30 mg/kg was also given before anti–PD-1 treatment in a separate cohort. LC used in this study consisted of polymers impregnated with chemotherapy that allow for a constant but not linear release of chemotherapy in the tumor microenvironment for at least 2 weeks. The majority of chemotherapy was delivered during the first week, with slower release of chemotherapy on the second week [see detailed kinetics in the study by Fleming et al. (10)].

To evaluate the immunological response of tumor-bearing mice to chemotherapy, we quantified the number of lymphocytes recovered from brain as well as blood, lymph nodes, and BM at various time points (Fig. 1). Mice treated with SC showed a decreased number of CD3^{+} lymphocytes compared to controls at the end of the first week of treatment, and this trend persisted over the course of treatment. At the end of the therapeutic regimen (day 30), SC-treated mice were severely lymphodepleted for at least 10 days after the end of treatment (LC versus SC, $P = 0.003$) (Fig. 1, day 41). The same lymphodepleting pattern was observed in the draining lymph nodes (DLNs). The SC group exhibited myelotoxicity, with lower overall cellularity of the BM as well as leukocytes (as measured by CD45) compared to the control (Fig. 1 and fig. S1). However, LC did not affect the number of TILs or lymphocytes in the peripheral lymphoid organs. Instead, we observed an increase in the number of TILs at a late time point (day 30) compared to SC or control mice (Fig. 1).

A small percentage of mice treated with SC or LC (30% versus 20%) were cured of disease and followed for 4 months after initial tumor implantation. Mice treated with high-dose SC showed a decreased number of recovered lymphocytes from lymph nodes ($P = 0.01$) and

[1]Department of Neurosurgery, Johns Hopkins University School of Medicine, Baltimore, MD 21287, USA. [2]Department of Oncology, Johns Hopkins University School of Medicine, Baltimore, MD 21287, USA. [3]Department of Neurosurgery, Seoul National University College of Medicine, Seoul 110-744, South Korea. [4]Department of Cancer Immunology, Johns Hopkins University School of Medicine, Baltimore, MD 21287, USA.
*These authors contributed equally to this work.
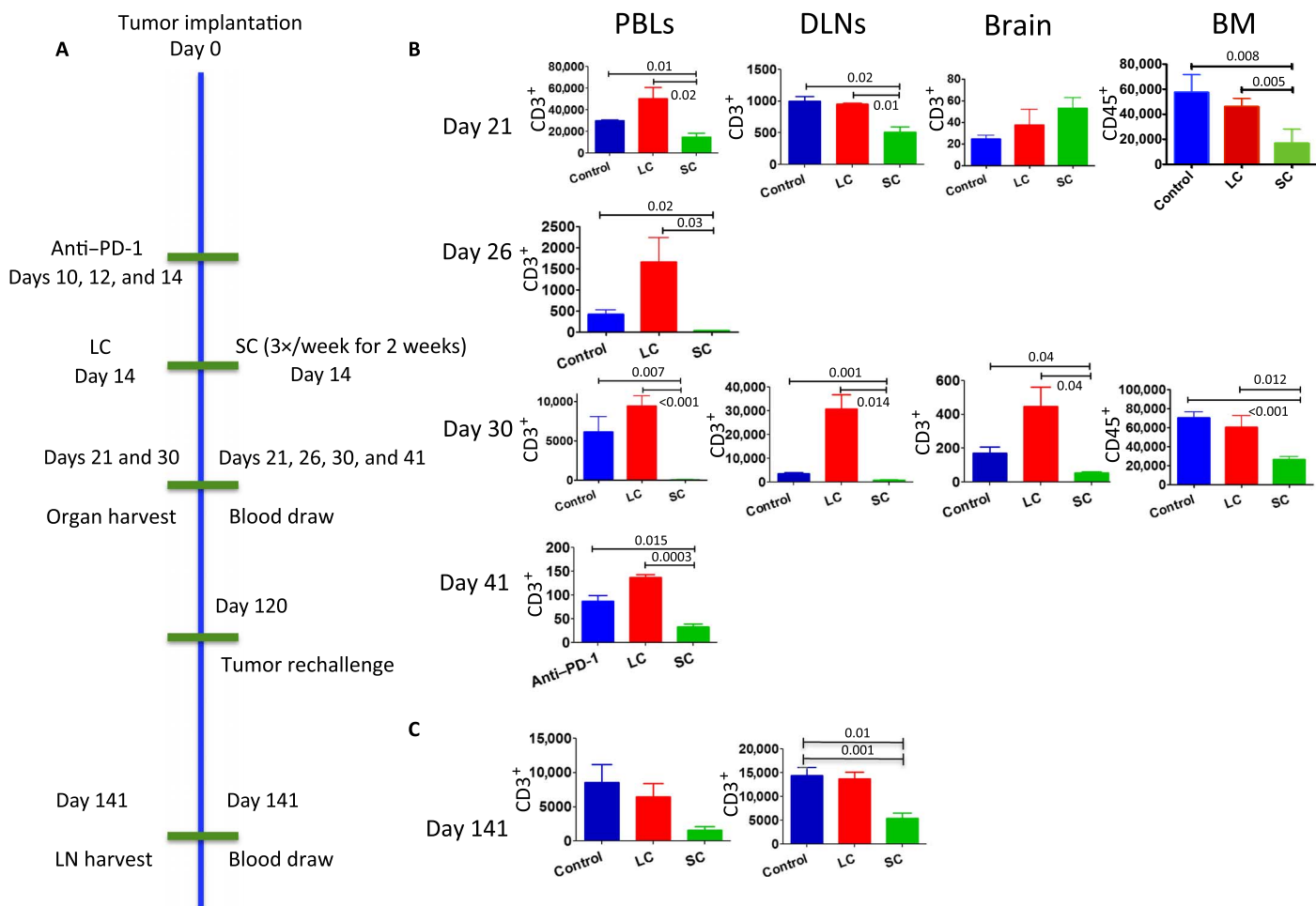†Corresponding author. Email: mlim3@jhmi.edu

Mathios et al., Sci. Transl. Med. 8, 370ra180 (2016)   21 December 2016

1 of 12

Fig. 1. SC resulted in severe and persistent lymphodepletion, whereas LC left the immune cell populations intact. (**A**) Experimental schedule: Mice were treated with either SC (intraperitoneal BCNU) or LC (BCNU polymers) at day 14. Intraperitoneal BCNU was given three times a week for 2 weeks. Flow analysis was performed for all groups for lymphocytes extracted from the brain, DLNs, and the peripheral blood at several time points ($n = 3$ for all graphs and all time points). Bar graphs show means ± 2 SD; P value was calculated by a two-sided Welch t test. LN, lymph node. (**B**) Early (days 21 and 26) lymphopenia and late (day 41) lymphopenia were observed in the peripheral blood of mice treated with SC. The same pattern was observed in the brain and the DLNs of mice treated with SC. SC-treated mice exhibited myelotoxicity (days 21 and 30), as indicated by the reduced BM cellularity and the reduced $CD45^+$ (leukocytes) population. (**C**) Persistent and potentially irreversible lymphopenia is observed in mice receiving high-dose SC. The T lymphocyte counts ($CD3^+$ cells) were decreased in the peripheral blood and the DLNs of mice [with long-term survival (LTS)] treated with SC compared to LC-treated mice or untreated (control) mice. PBL, peripheral blood lymphocyte.

blood ($P = 0.07$) compared to untreated or LC-treated mice, even at the 4-month mark (Fig. 1).

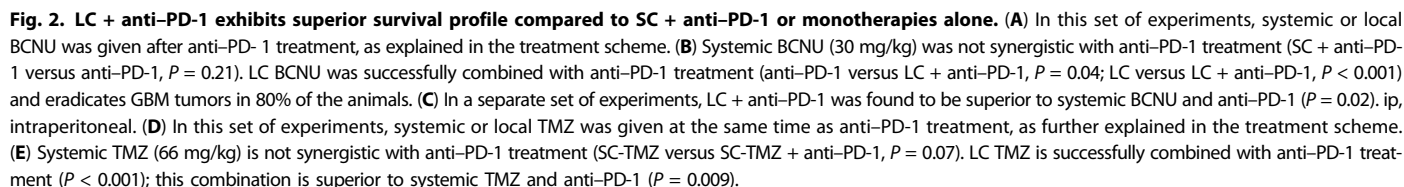## The use of SC is inferior compared to combined LC and anti–PD-1 treatment

The delivery method of chemotherapy in tumor-bearing mice had a marked effect on immune function. SC produced severe lymphopenia in the peripheral lymphoid organs and the tumor microenvironment, whereas LC did not. In light of these findings, we evaluated whether LC or SC (BCNU) is superior in combination with anti–PD-1. LC alone increased survival compared to the empty polymer (EP; wafer without chemotherapeutic agent) group ($P = 0.028$). No difference in survival was seen in SC compared to LC ($P = 0.41$). The combination of SC + anti–PD-1 resulted in similar survival compared to anti–PD-1 alone ($P = 0.4$). LC + anti–PD-1 had the greatest survival benefit, when compared to anti–PD-1 alone ($P = 0.03$), and was superior to LC alone ($P < 0.001$) (Fig. 2A). In

a large cohort of mice (15 mice per group), LC + anti–PD-1 exhibited higher survival rates compared to SC + anti–PD-1 ($P = 0.03$) (Fig. 2A, bottom). IVIS imaging of the mice in this cohort (fig. S2) showed that mice treated with anti–PD-1 had a quick tumor regression, unlike the mice treated with SC, which had persistent tumor for up to 60 days before they died.

The concomitant use of high-dose systemic TMZ with anti–PD-1 failed to show synergism; combination of systemic TMZ with anti–PD-1 was inferior to the combination of high-dose local TMZ with anti–PD-1 ($P = 0.009$). The use of high-dose LC was synergistic in combination with anti–PD-1 treatment (LC versus LC + anti–PD-1, $P = 0.0049$; anti–PD-1 versus LC + anti–PD-1, $P < 0.001$; Fig. 2B).

Addition of SC to anti–PD-1 treatment results in severe lymphodepletion

LC-treated mice showed an increased number of $CD3^+$ lymphocytes compared to the control group in the peripheral blood (day 30;

Mathios *et al.*, *Sci. Transl. Med.* **8**, 370ra180 (2016)   21 December 2016

2 of 12

Fig. 2. LC + anti–PD-1 exhibits superior survival profile compared to SC + anti–PD-1 or monotherapies alone. (**A**) In this set of experiments, systemic or local BCNU was given after anti–PD- 1 treatment, as explained in the treatment scheme. (**B**) Systemic BCNU (30 mg/kg) was not synergistic with anti–PD-1 treatment (SC + anti–PD-1 versus anti–PD-1, P = 0.21). LC BCNU was successfully combined with anti–PD-1 treatment (anti–PD-1 versus LC + anti–PD-1, P = 0.04; LC versus LC + anti–PD-1, P < 0.001) and eradicates GBM tumors in 80% of the animals. (**C**) In a separate set of experiments, LC + anti–PD-1 was found to be superior to systemic BCNU and anti–PD-1 (P = 0.02). ip, intraperitoneal. (**D**) In this set of experiments, systemic or local TMZ was given at the same time as anti–PD-1 treatment, as further explained in the treatment scheme. (**E**) Systemic TMZ (66 mg/kg) is not synergistic with anti–PD-1 treatment (SC-TMZ versus SC-TMZ + anti–PD-1, P = 0.07). LC TMZ is successfully combined with anti–PD-1 treatment (P < 0.001); this combination is superior to systemic TMZ and anti–PD-1 (P = 0.009).

Fig. 3A), or to anti–PD-1 (fig. S3A). The combination of SC + anti–PD-1 exhibited a similar lymphodepleting profile to SC treatment alone: CD3$^+$ blood lymphocytes started decreasing at day 21 (P < 0.001; Fig. 3A and fig. S3A) and reached the same levels as mice treated with SC alone (P = 0.9; Fig. 3). Mice treated with the combination of LC + anti–PD-1 maintained a high number of circulating lymphocytes compared to the nontreated mice (P = 0.5; Fig. 3A and fig. S3).

Flow cytometric analysis of the DLNs confirmed lymphodepletion of both CD3$^+$ cells and CD8$^+$IFN-γ$^+$ cells in the SC and SC + anti–PD-1 groups. Anti–PD-1, LC, and combination of LC + anti–PD-1 groups had higher numbers of CD3$^+$ and higher percentages of CD8$^+$IFN-γ$^+$ cells compared to the control. The combination treatment resulted in a higher percentage of CD8$^+$IFN-γ$^+$ cells compared to monotherapies (anti–PD-1 versus LC + anti–PD-1, P = 0.02; LC versus LC + anti–PD-1, P = 0.03; fig. S3B). The percentage of CD4$^+$FoxP3$^+$ cells decreased in all treatment groups compared to the control, including the groups treated with SC.

Additionally, we found that mice in the SC group showed a significant decrease in the cellularity of the BM (P = 0.0185) on the basis of viability dye staining. The addition of anti–PD-1 failed to reconstitute the cellularity of the BM (P = 0.0079). The analysis of CD45$^+$ BM cells (leukocytes) from the SC and SC + anti–PD-1 groups revealed decreased live cell numbers compared to the control, LC, or LC + anti–PD-1 groups (P = 0.03) (fig. S1, A and B). A more detailed analysis of the BM cell subpopulations indicated that SC + anti–PD-1 exhibited an increased percentage of granulocytic cells (fig. S1, B and C).

Addition of SC to anti–PD-1 treatment results in severe depletion of TILs

Mice were sacrificed at days 21 and 30, and TILs were analyzed to assess the effects of each treatment regimen on lymphocytes present in the tumor microenvironment. The percentage and number of CD4$^+$FoxP3$^+$ regulatory cells were higher in SC compared to the control (53.6% versus 29.3%, P = 0.02). LC moderately increased the percentage of T$_{reg}$ cells
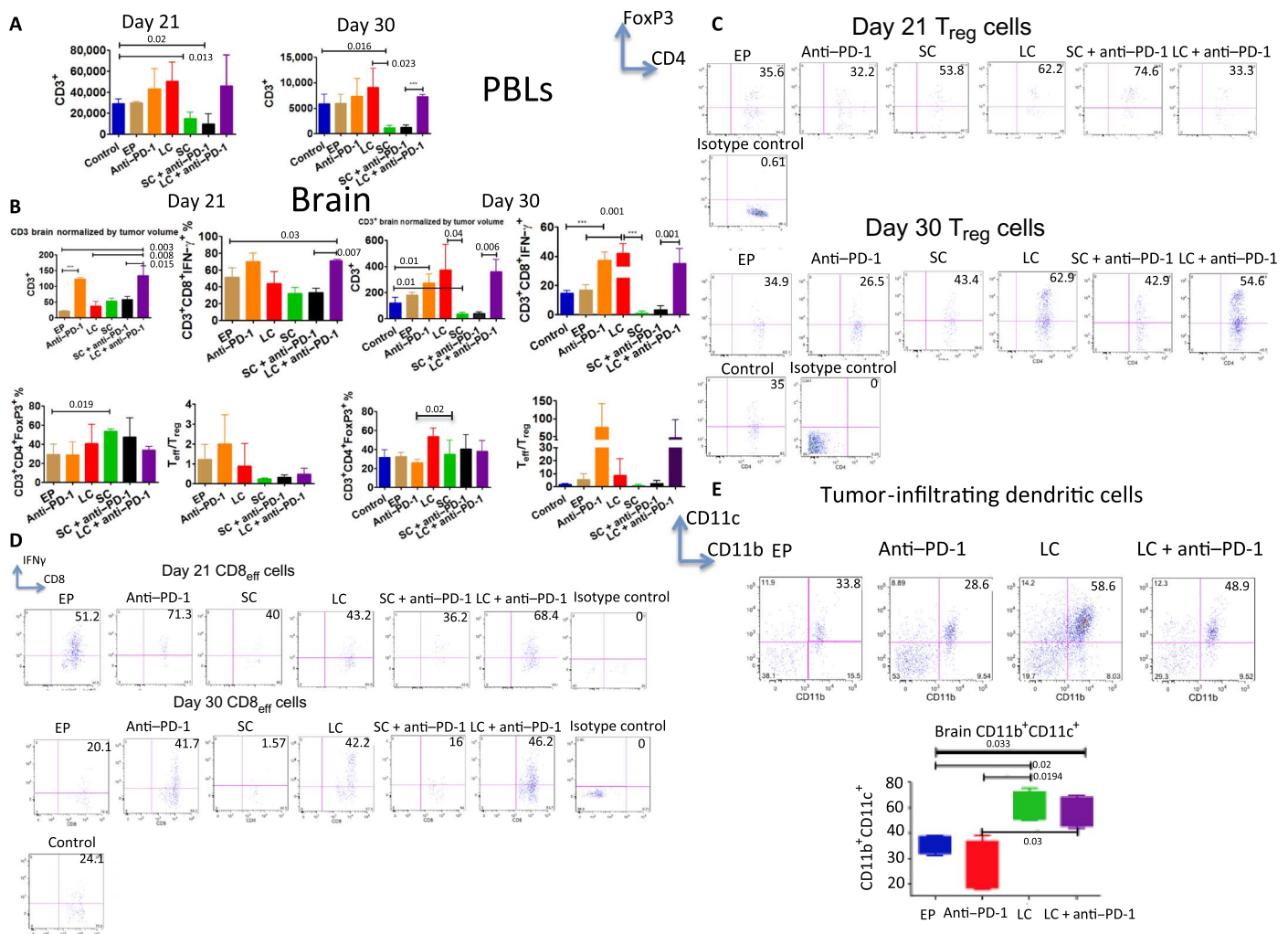
Fig. 3. **LC + anti–PD-1 elicits a robust immune response, whereas SC + anti–PD-1 abrogates immune activation the anti–PD-1 alone creates.** (**A**) SC in combination with anti–PD-1 resulted in lymphopenia in the peripheral blood, whereas LC + anti–PD-1 maintained high lymphocyte counts at all time points ($n = 3$ for all treatment groups). Bar plots show means ± 2 SD. P values were calculated on the basis of two-tailed Welch test. (**B** to **D**) At day 21, LC + anti–PD-1 resulted in high numbers of TILs and increased percentage of T effector (T_{eff}) cells compared to SC + anti–PD-1 or LC alone. At day 30, SC groups showed lymphodepletion and decreased T_{eff} function (decreased IFN-γ production). However, LC increased the T_{eff} function, resulting in an increased ratio of T_{eff}/T regulatory (T_{reg}) cells. Flow cytometry plots show results from a single mouse for each group. (**E**) Box-and-whiskers plot and flow cytometry charts illustrating the percentage of tumor-infiltrating dendritic cells; gating on the CD45+ cells (leukocytes) infiltrating the brain and focusing on the CD11b+CD11c+ cells (dendritic cells). We observed an increased infiltration of dendritic cells in the LC-treated mice.

(40%) versus EP. Animals treated with anti–PD-1 had the same percentage of T_{reg} cells as the control ($P = 0.96$). The addition of anti–PD-1 to LC moderately decreased the number of CD4+FoxP3+ cells (34.2%), close to the number in control mice (Fig. 3, B and C), but did not significantly decrease the percentage of T_{reg} cells in combination with SC (47.6%, $P = 0.64$) (Fig. 3, B and C).

At day 21, 51.7% of the CD8+ cells recovered from control mice produced interferon-γ (IFN-γ). The LC and SC groups exhibited a similar percentage of CD8+IFN-γ+ cells, with 44 and 34% of the recovered CD8+ cells producing IFN-γ, respectively ($P = 0.5$ and $P = 0.15$). The addition of anti–PD-1 antibody to LC treatment increased the percentage of CD8+IFN-γ–producing cells to 71% ($P = 0.03$), which was similar to anti–PD-1 alone ($P = 0.87$; Fig. 3, B and D).

At day 30 after tumor implantation, the density of CD3+ TILs (normalized to tumor volume) in the SC group was significantly less than the control (40 cells versus 140 cells, $P < 0.001$). LC enhanced the per-

centage and number of CD8+IFN-γ–producing cells (42%, 80 cells) compared to the control (15%, 30 cells; $P < 0.001$). LC + anti–PD-1 had a higher percentage of CD8+IFN-γ–producing cells (38%) compared to the control (15%, $P < 0.001$) but similar percentage compared to LC (42%, $P = 0.38$) or anti–PD-1 alone (38%, $P = 0.75$). The percentage of CD4+FoxP3+ cells was similar at day 30 among control (31.6%), EP (32.4%), and anti–PD-1 (26%) groups. LC continued to have a higher percentage of T_{reg} cells (53.6%) compared to EP (32.4%, $P = 0.02$), but the combination of LC + anti–PD-1 restored the percentage of CD4+FoxP3+ cells (37%) to that of the control ($P = 0.1$) (Fig. 3, B and C).

LC enriches tumor-infiltrating dendritic cells without affecting microglia and tumor-associated macrophages

Resident microglia were identified as CD11b+CD45^{low}, infiltrating macrophages-monocytes as CD11b+CD45^{high}, and TILs as CD11b−CD45^{high} cells. The relative percentages of lymphocytes,

microglia, and monocytes exhibited variability among groups, with no distinct pattern for any specific group (fig. S4, A and B). However, the lymphocyte/microglia ratio strongly correlated with tumor size ($P = 0.003$, $r^2 = 0.79$) (fig. S4C). Further analysis of the tumor-infiltrating macrophages showed no distinct pattern among different groups; however, a positive correlation existed between tumor size and monocyte/granulocyte ratio ($P = 0.046$, $r^2 = 0.5$; fig. S5C).

Tumor-infiltrating dendritic cells, defined as $CD11b^+CD11c^+$ cells gated from the population of $CD45^+$ cells, showed an increased percentage in the LC and LC + anti–PD-1 groups compared to the EP or anti–PD-1 groups (Fig. 3E). This result suggests that LC pro-

moted infiltration of the tumor microenvironment with peripheral dendritic cells.

Reversing the sequence of SC and immunotherapy abrogates survival benefit of immunotherapy

To investigate whether the sequence of immunotherapy and chemotherapy affects survival, we delivered chemotherapy before immunotherapy. Again, we observed that LC mice trended toward a longer survival compared to EP ($P = 0.07$). Despite the use of chemotherapy (LC or SC) at an earlier time point (day 7) (Fig. 4A), the median and long-term survival did not change compared to results seen in the initial
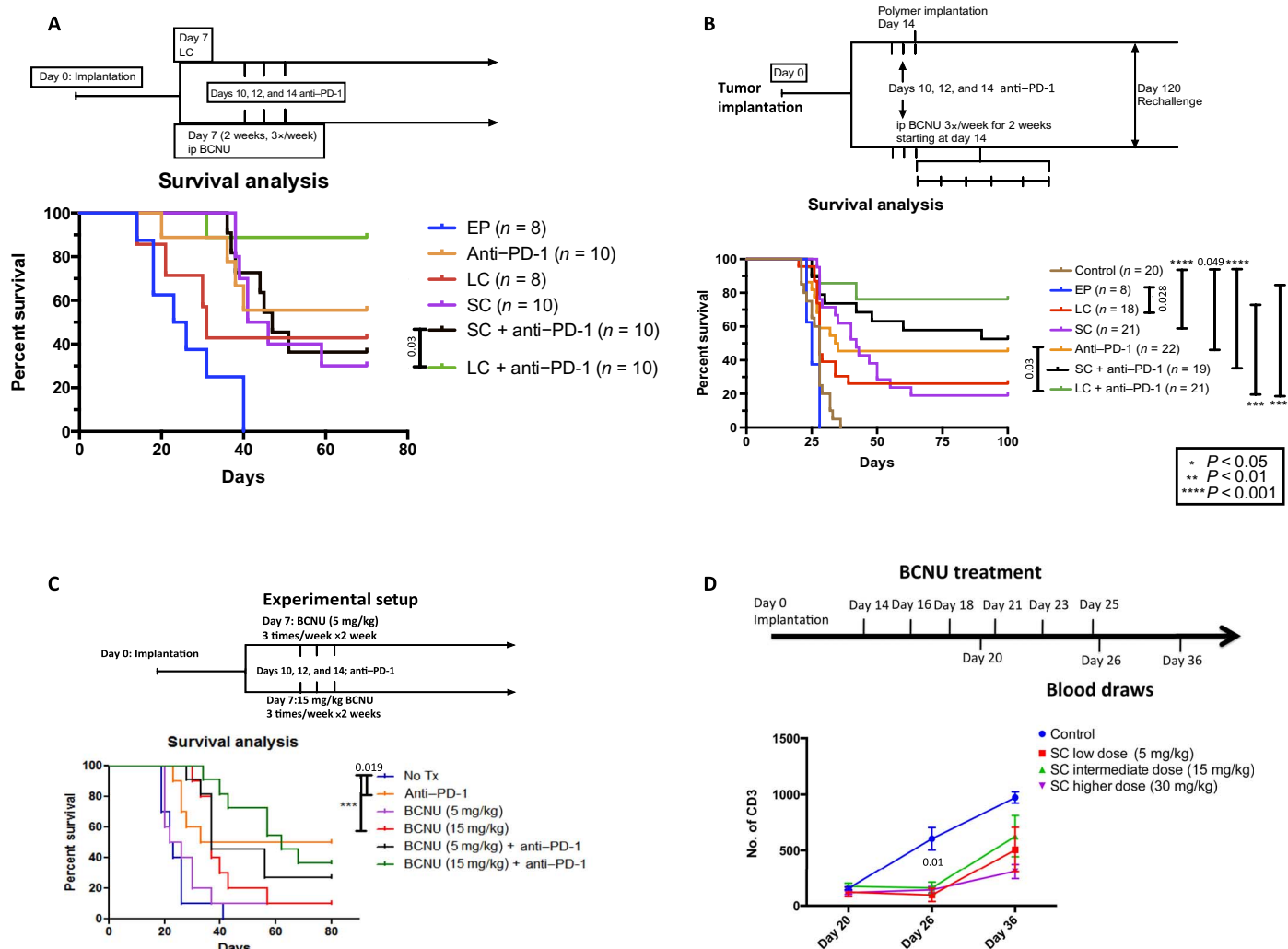
Fig. 4. SC given before anti–PD-1 treatment abrogates the survival benefit of anti–PD-1. (**A**) Timeline and survival curve of anti–PD-1 administration after chemotherapy (dose of 30 mg/kg). The use of SC (day 7) before starting treatment with anti–PD-1 (day 10) resulted in a decreased LTS rate (30%) compared to anti–PD-1 treatment alone (50%). (**B**) Timeline and survival curve of anti–PD-1 before chemotherapy administration. When SC was given after anti–PD-1, it did not negatively affect LTS induced by anti–PD-1. In both sequencing scenarios, LC + anti–PD-1 was superior to SC + anti–PD-1 (chemotherapy after anti–PD-1 treatment). (**C**) Timeline and survival curve for BCNU titration experiments: BCNU was given before treatment with anti–PD-1. Two different doses of systemic BCNU treatment failed to show synergism between SC and anti–PD-1 treatment. The use of low-dose BCNU (5 mg/kg) did not show survival differences compared to the untreated (No Tx) group. The use of intermediate-dose BCNU (15 mg/kg) showed survival benefit compared to the No Tx group ($P < 0.001$). However, both the BCNU (5 mg/kg) + anti–PD-1 and BCNU (15 mg/kg) + anti–PD-1 groups showed no synergism with anti–PD-1 treatment. (**D**) Timeline and flow cytometric analysis of PBLs from the BCNU titration experiments. On day 20, no significant differences were observed in the number of lymphocytes among the BCNU groups and the control group. On day 26, 1 day after completion of the BCNU treatment course, all treatment groups exhibited a significantly ($P = 0.01$) lower number of PBLs compared to the control group. The difference in the number of PBLs was maintained on day 36, 11 days after the end of chemotherapy treatment, for the high-dose (30 mg/kg) group ($P = 0.002$) but not for the other chemotherapy groups. The figure shows means ± 2 SD values ($n = 4$) for each treatment group.

experiments, where immunotherapy was delivered before chemotherapy (day 14) (Fig. 4B). The order of treatment similarly did not change outcomes, and LC before or after anti–PD-1 administration generated similar survival data (90% versus 80% LTS) (Fig. 4, A and B). However, when combining anti–PD-1 with SC, the survival benefit of anti–PD-1 was abrogated by giving chemotherapy first (30% versus 50% LTS) (Fig. 4A). These results are in contrast to our first round of experiments (SC given after anti–PD-1), where SC + anti–PD-1 exhibited similar survival as anti–PD-1 alone (55% versus 50% LTS; Fig. 4B). Furthermore, the combination of anti–PD-1 and LC showed a significantly better survival ($P = 0.03$) compared to anti–PD-1 and SC, consistent with our observations from the previous experiment, where chemotherapy was given after the end of immunotherapy (Fig. 4, A and B).

SC lacks synergism with anti–PD-1 treatment independent of treatment dose

We titrated the dose of systemic BCNU to assess whether low-dose (5 mg/kg), intermediate-dose (15 mg/kg), or high-dose (30 mg/kg) SC can be effectively combined with anti–PD-1. All BCNU regimens failed to show synergism with anti–PD-1. Specifically, low dose (5 mg/kg) + anti–PD-1 showed no difference in overall survival compared to anti–PD-1 alone ($P = 0.37$) (Fig. 4C). The intermediate dose (15 mg/kg) + anti–PD-1 also failed to show any difference in overall survival compared to anti–PD-1 ($P = 0.92$); it furthermore exhibited decreased LTS (36.3%) compared to anti–PD-1 (Fig. 4C). Last, the high-dose (30 mg/kg) treatment showed lack of synergism ($P = 0.64$) with anti–PD-1 and decreased LTS in the high dose (30 mg/kg) + anti–PD-1 group (30%) compared to anti–PD-1 (Fig. 4A). Flow cytometry of the peripheral blood drawn on days 20, 26, and 36 after implantation demonstrated a considerable decrease in the total number of circulating CD3 cells in the high-dose (30 mg/kg) BCNU group and a transient decrease in the low-dose (5 mg/kg) and intermediate-dose (15 mg/kg) groups on day 26 (Fig. 4D). Of note, there was no significant difference among the three treatment groups in the percentage of lymphodepletion across the experimental time points [two-way analysis of variance (ANOVA) ($P = 0.4$ for treatment groups, $P = 0.001$ for time variable)].

LC and anti–PD-1 increase homing of tumor antigen-specific T cells in tumor compared to SC

We intracranially implanted mice with GL261 OVA cells and adoptively transferred lymphocytes from OT-I mice modified to express a T cell receptor with high affinity for the ovalbumin residues 257 to 264 in the context of H2Kb MHC-I (H-2Kb major histocompatibility complex class I) peptide. Four days after adoptive transfer and 3 days after initiation of chemotherapy, we harvested DLNs and brains of animals implanted with GL261 OVA tumors. Flow analysis with CD3 and CD45.2 markers showed that LC + PD-1 increased the percentage and number of adoptively transferred OVA-specific (CD45.2) T cells residing in the DLNs and the tumor microenvironment compared to SC or anti–PD-1 (Fig. 5). These profiles were more exaggerated within the tumor microenvironment compared to the DLNs; mice treated with LC + anti–PD-1 had a significantly higher percentage of $CD3^+CD45.2^+$ cells in the tumor microenvironment compared to anti–PD-1 (23% versus 8%, $P = 0.0343$) as well as to SC + anti–PD-1 (23% versus 6%, $P = 0.026$) treatment. Furthermore, LC had a significantly higher percentage of $CD3^+CD45.2^+$ cells compared to SC ($P = 0.0329$). These data suggest that LC indeed increases antigen-specific immune activity in the tumor.

LC preserves memory response against rechallenge, whereas SC abrogates memory response

To assess memory response, mice with LTS were rechallenged with GL261 cells, and naïve mice were challenged in parallel. No tumor growth occurred in the anti–PD-1, LC, and LC + anti–PD-1 groups, indicating a memory response upon tumor antigen recognition. In contrast, naïve mice developed large, progressively growing tumors. LTS in the SC or SC + anti–PD-1 groups also developed large, progressively growing tumors after tumor rechallenge (Fig. 6, A and B).

Twenty days after intracranial tumor rechallenge, mice with LTS were assessed for the presence of memory cells. $CD3^+CD8^+CD44^{[high]}CD62L^{[low]}$ cells were considered T effector memory (TEM) cells, and $CD3^+CD8^+CD44^{[low]}CD62L^{[high]}$ as T central memory (TCM) cells. Whereas mice treated with anti–PD-1, SC, or LC + anti–PD-1 exhibited similar percentages of $CD4^+$ or $CD8^+$ TCM and TEM cells, the TEM cells from the SC group were dysfunctional. IFN-γ production after stimulation with phorbol 12-myristate 13-acetate/ionomycin in TEM cells isolated from DLNs, spleen, or peripheral blood was lower in SC than in anti–PD-1 or LC + anti–PD-1 (Fig. 6, C and D).

The abovementioned data indicate that the immune memory response to anti–PD-1 treatment was abrogated by adding high-dose SC (Fig. 6, A to C). In Fig. 6E, we show that moderate dose of systemic BCNU also abrogates memory immune response. More specifically, nine of nine mice treated with BCNU (30 mg/kg) + anti–PD-1 redeveloped tumor after tumor rechallenge and died from it; one of one mouse treated with BCNU (15 mg/kg) redeveloped the tumor and died from it; and three of three mice treated with BCNU (15 mg/kg) + anti–PD-1 developed the tumor (two of three died from it).

To identify whether the presence of intact CD8 memory cells could allow SC + anti–PD-1 mice to regain their ability to reject the tumor after rechallenge, we harvested CD8 cells from spleens of mice treated with LC + anti–PD-1 and adoptively transferred them into mice treated with SC + anti–PD-1 and rechallenged with tumor, as described in fig. S5A. As mentioned, mice treated with SC + anti–PD-1 and rechallenged with tumor failed to reject the tumor and quickly grew large tumors. These tumors were well established when CD8 cells were adoptively transferred (day 12). Two of the four recipient mice (50%) showed a transient decrease in the bioluminescent signal after adoptive transfer of CD8 cells (fig. S5, A and B). We observed that adoptively transferred effector CD8 cells were able to slow the progression of the tumor but not completely eradicate recurrent tumors. This suggests that adoptive transfer of memory CD8 cells is not adequate to maintain a durable immune response.

In separate experiments, mice with LTS from the SC group were rechallenged with tumor (SC R) and treated with anti–PD-1. Control mice implanted with primary tumor and treated with anti–PD-1 exhibited 50% LTS as expected, whereas mice originally treated with SC for their primary tumor and treated with anti–PD-1 for their rechallenged tumor (SC R + postrechallenge anti–PD-1) failed to respond to anti–PD-1 (Fig. 7A). Additionally, the rate of tumor progression in the SC R + postrechallenge anti–PD-1 group, as measured by bioluminescent imaging, was similar to the rate in tumor-bearing mice that did not receive treatment (Fig. 7A). Harvested peripheral blood and brain of these rechallenged mice confirmed that T memory cells from the SC + anti–PD-1 mice exhibited dysfunctional IFN-γ production (Fig. 7, B and C) compared to the LC + anti–PD-1 mice. Furthermore, we observed that anti–PD-1 in the SC R mice did not restore the functionality of memory T cells. More specifically, T memory cells in the brain parenchyma of mice
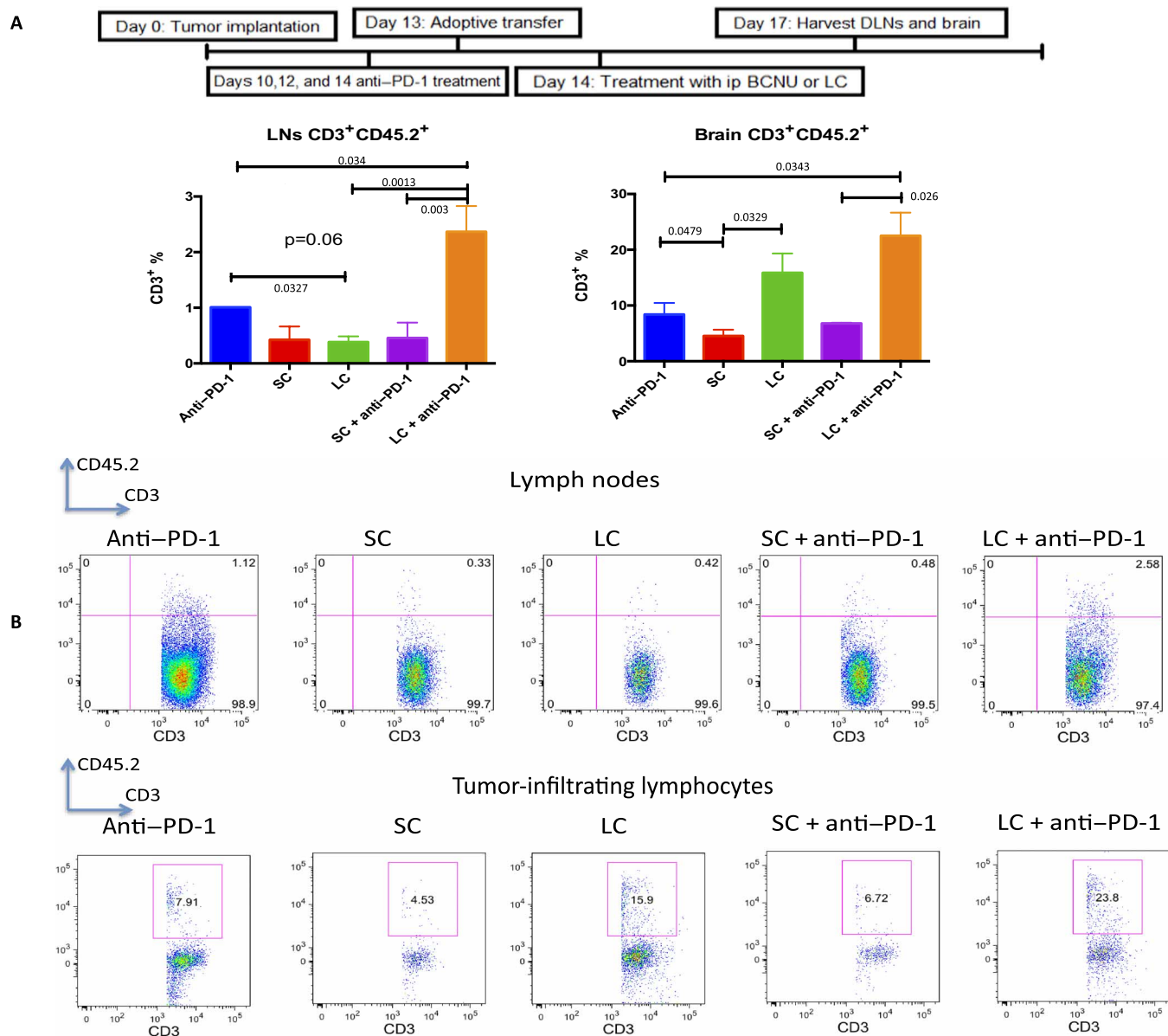
Fig. 5. The combination of LC + anti–PD-1 stimulated expansion of antigen-specific T cells intratumorally and in the DLNs. (**A**) B6 mice expressing the congenic marker CD45.1 were implanted with GL261 cells and were treated with anti–PD-1 (days 10 to 14) and SC or LC (starting at day 14). Spleen lymphocytes from OT-I mice expressing the congenic marker CD45.2 were adoptively transferred at day 13 into the tumor-bearing mice. At day 17 (4 days after adoptive transfer), CD45.2$^+$ cells were recovered from recipient mice. (**B**) We observed an expansion of OT-I T cells in the LC + anti–PD-1 group compared to the anti–PD-1, SC, or SC + anti–PD-1 groups. Graphs show means ± 2 SD, and P values were calculated with a two-tailed Welch test.

treated with LC + anti–PD-1 showed markedly higher IFN-γ production compared to SC R and rescue anti–PD-1 (70% versus 20%, $P = 0.02$). The same patterns of IFN-γ production from T memory cells were observed in peripheral blood, with LC and anti–PD-1 exhibiting the highest T memory–associated IFN-γ production (Fig. 7, B and C). After performing necropsies on these mice on experimental day 104, we observed that the size of the spleen in the SC-treated mice was significantly decreased compared to the mice treated with LC + anti–PD-1 ($P = 0.003$; Fig. 7D). Figure 7D shows visual proof of tumor regrowth in the SC-treated groups and absence of tumor regrowth in the LC + anti–PD-1 group.

DISCUSSION
Although chemotherapy and immunotherapy have been widely used and validated independently, combination therapy has been controversial because of known immunosuppressive effects of chemotherapy. Recently, efforts have been undertaken to identify conditions under which chemotherapy can potentiate the use of immunotherapy. The doses, delivery methods, and types of chemotherapy and immunotherapy can drastically alter outcomes (11). Certain chemotherapies seem to have differential effects on specific lymphoid subsets, as in the case of cyclophosphamide, which preferentially depletes T$_{reg}$ cells in low doses (12). The type of cell death may also affect immune
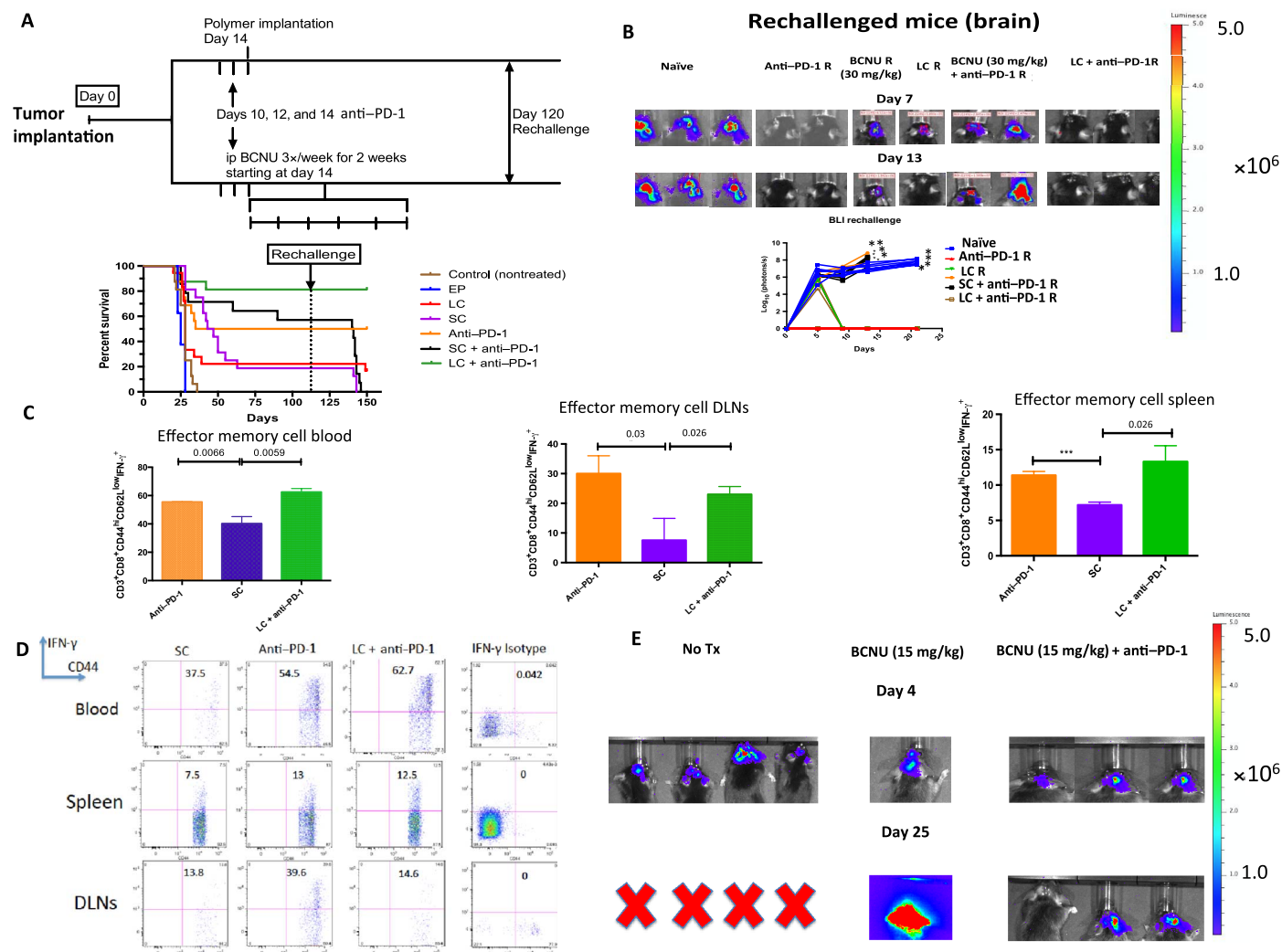
Fig. 6. SC abrogated the antitumor memory response in mice treated with anti–PD-1 and resulted in a functional impairment of T memory cells. (A) The treatment scheme shows the initial treatment schedule as well as the timing of the rechallenge. Mice with LTS from all groups were rechallenged; mice in the LC groups and the anti–PD-1 group had no tumor recurrence, whereas SC-treated mice failed to reject the rechallenged tumor and died. **(B)** The figure shows representative mice from each group (naïve, $n = 5$; anti–PD-1, $n = 5$; SC, $n = 3$; LC, $n = 3$; SC + anti–PD-1, $n = 3$; LC + anti–PD-1, $n = 5$). Rechallenged mice were followed with bioluminescent imaging; the plot shows the tumor signal, as measured by photons per second. Mice treated with SC or SC + anti–PD-1 exhibited progressively increasing signal and eventually died of their tumor, as denoted by the asterisk at the end of the line for each mouse. Mice treated with anti–PD-1 rejected the tumor right away, showing no tumor signal at any time point, whereas LC and LC + anti–PD-1 had a transient tumor signal at day 5 that was eliminated by day 7. **(C and D)** The percentage of effector CD8 memory cells producing IFN-γ was lower in the SC-treated mice than in other groups across all peripheral tissues, including the spleen, peripheral blood, and DLNs. **(E)** Mice with LTS from the intermediate-dose (15 mg/kg) ($n = 1$) and the intermediate-dose (15 mg/kg) + anti–PD-1 ($n = 3$) groups were rechallenged with GL261 LUC cells in the brain. As with the higher BCNU dose (30 mg/kg), the intermediate-dose (15 mg/kg) groups failed to produce an immune memory response. The rechallenge experiment with the alternative doses of BCNU was run only once.

stimulation. It has been hypothesized that treatments resulting in apoptosis are less effective in inducing a robust immune response because apoptosis abrogates tumor antigen presentation, whereas necrosis results in antigen release (8).

The experiments described here serve as evidence that LC in the form of controlled-release BCNU or TMZ polymers is superior to SC in potentiating anti–PD-1–mediated antitumor immune response. This regimen provides a robust survival benefit as well as increased tumor-infiltrating immune cells and memory cells necessary to resist tumor rechallenge (Fig. 8). These results highlight the importance of rigorously testing the effects of order, timing, and delivery method in implementing combination chemotherapy/immunotherapy regimens.

We found that LC not only allowed for retained activity of anti–PD-1 but also boosted immune response. One potential mechanism may be increased antigen presentation as tumor cells die in response to chemotherapy. This hypothesis is supported by the increased percentage of dendritic cells present in the LC groups compared to the control or anti–PD-1 groups. Tumor-infiltrating dendritic cells are potent antigen-presenting cells (13, 14). By implanting GL261 OVA cells in mice and adoptively transferring OT-I lymphocytes, we observed that LC allowed for greater expansion of the adoptively transferred OVA-specific lymphocytes in the brain compared to mice treated with anti–PD-1 alone or SC + anti–PD-1. These results support the hypothesis that LC-induced cell death attracts more dendritic cells that take up released antigens,
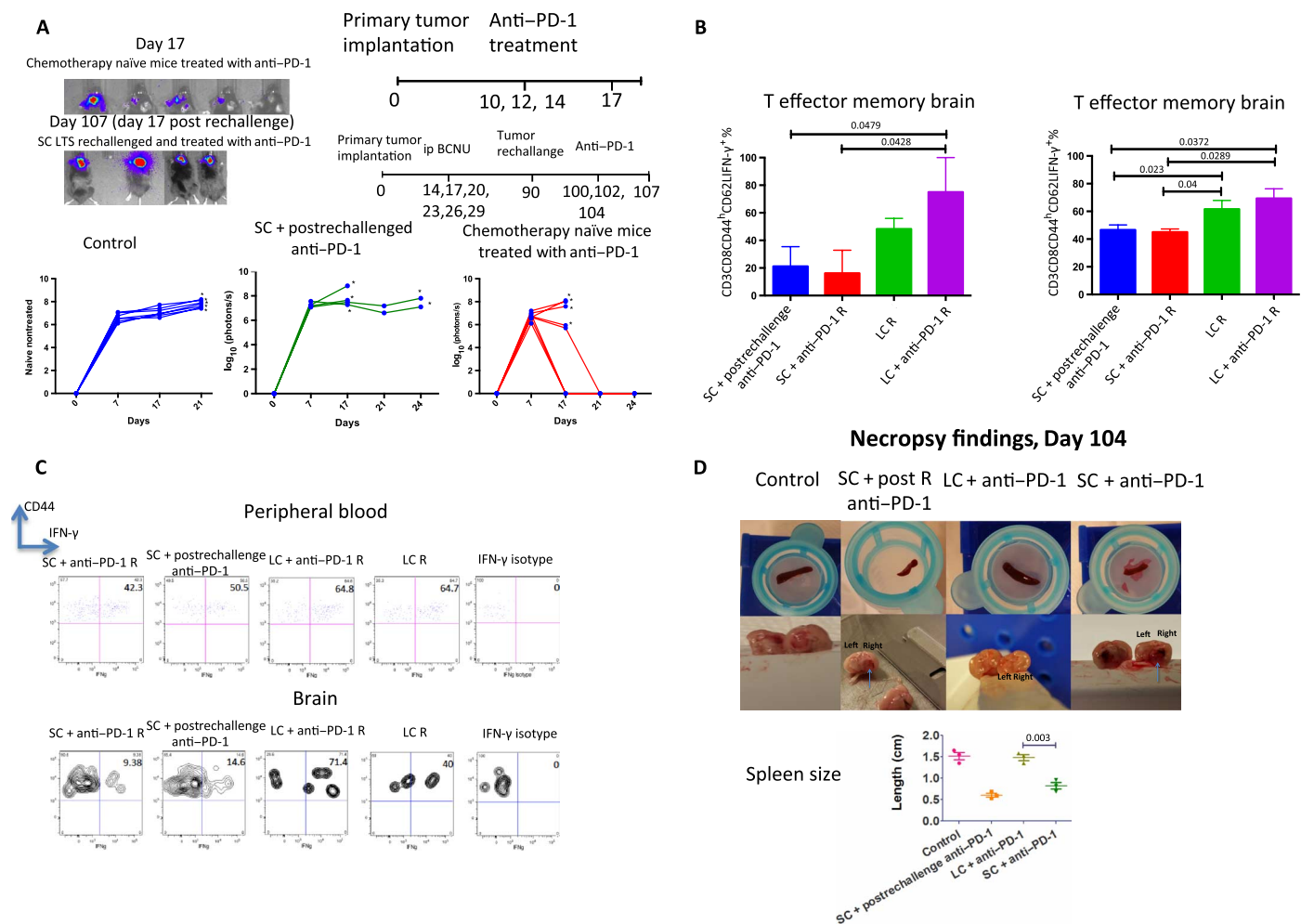
Fig. 7. Prior use of SC mutes antitumor immune response of anti–PD-1. (**A**) Mice from the SC group with recurrent tumor after rechallenge were treated with anti–PD-1. Chemotherapy naïve mice were also treated with anti–PD-1. IVIS imaging after treatment shows tumor progression in both treatment groups. Rechallenged SC-treated mice received their last dose of SC more than 2 months before subsequent treatment with anti–PD-1. All of the SC-treated mice developed recurrent tumors despite treatment with anti–PD-1, whereas only 50% of the chemotherapy naïve mice developed tumor with anti–PD-1 treatment. (**B** and **C**) After gating T cells for CD8^{+}CD62L^{low}CD44^{high} to identify the TEM cells, we assessed their activation status by looking for IFN-γ production upon stimulation. TEM activation in mice treated with SC was decreased despite anti–PD-1 treatment. (**D**) Upon necropsy, mice that had received SC and were later (after rechallenge) treated with anti–PD-1 or mice treated with SC + anti–PD-1 exhibited much smaller spleens than the untreated or LC + anti–PD-1 mice. Furthermore, mice treated with SC and then rechallenged with tumor on the contralateral hemisphere (right side) had large tumors, unlike the mice treated with LC and rechallenged with anti–PD-1 that exhibited no tumor recurrence.

allowing for greater antigen presentation and further clonal activation of tumor-specific T cell responses. In contrast, the use of SC seems to abrogate antitumor antigen-specific T cell responses. The effect of LC versus SC on tumor-infiltrating dendritic cells will require future characterization. Establishing the exact mechanism of increased antigen presentation after LC will require additional experiments because increased antigen-specific tumor responses can result from LC effects on multiple levels (cellular, antigen-processing machinery, and antigen affinity). Furthermore, LC did not seem to increase tumor-specific T cells in the DLNs, unlike in the tumor microenvironment where it enhanced T cell expansion more than anti–PD-1 alone. We hypothesize that this difference in T cell expansion in the tumor microenvironment but not DLNs could be a result of antigen presentation occurring in the tumor more than in the DLNs or possibly due to disruption of the blood-brain barrier by LC and further infiltration of T cells in the tumor. We realize, though, that our results only show a snapshot of these events

and that future more detailed experiments are required to identify the location of antigen presentation.

These immunologic findings are consistent with our survival data. Combination LC and anti–PD-1 exhibited the most robust survival benefit compared to control and monotherapy. Furthermore, these data show that SC does not work synergistically with anti–PD-1. These results are independent of the chemotherapy agent, concentration of local or SC, and the timing of SC in relation to immunotherapy. The use of SC alone or in combination with anti–PD-1 resulted in delayed tumor progression compared to control or anti–PD-1, respectively; however, the tumors recurred, resulting in late mortality. Consistent with these data are the results of the survival experiment where SC was given before immunotherapy; addition of SC to anti–PD-1 did not provide a survival benefit and was inferior to PD-1 monotherapy.

The combination of LC and anti–PD-1 enhanced antitumor immune response within the tumor microenvironment, further supporting the
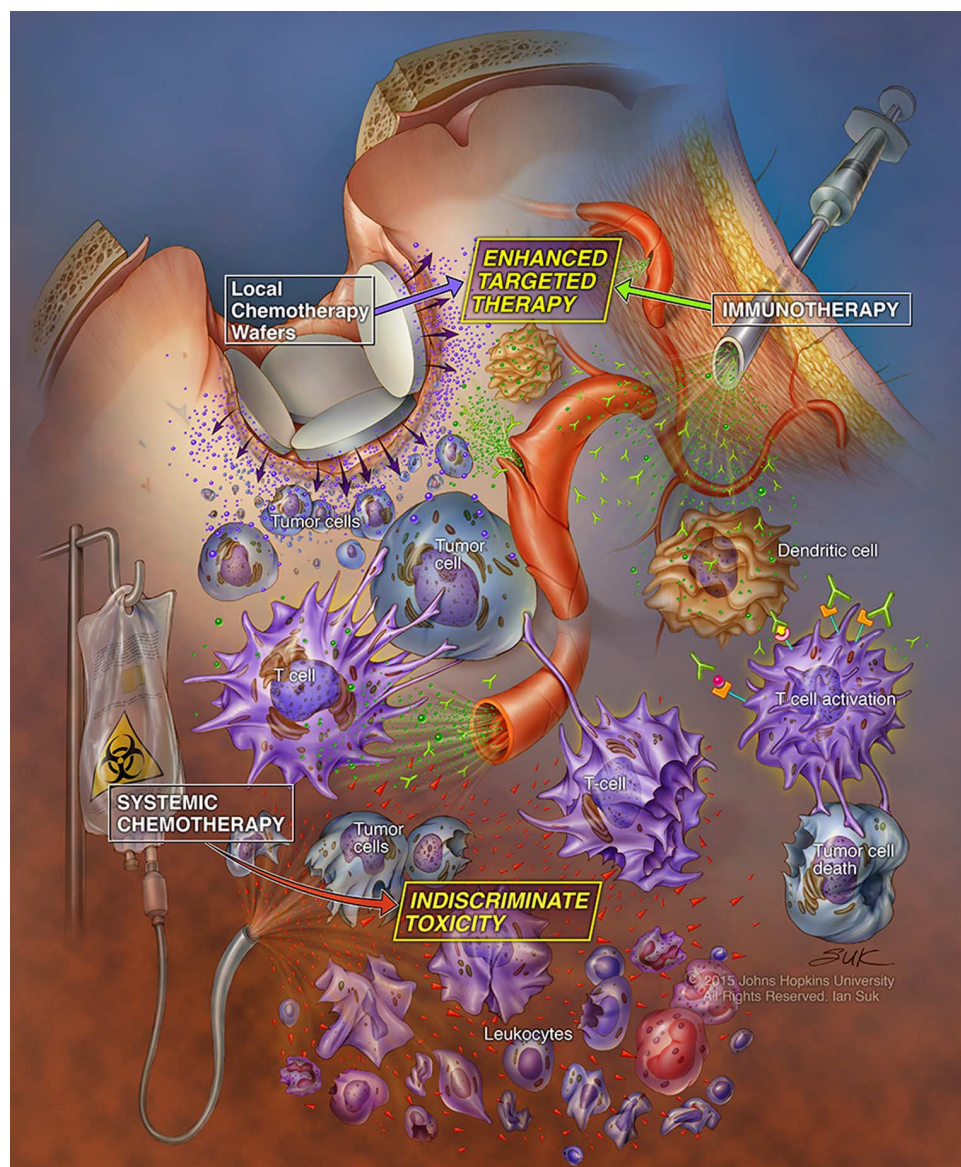
Fig. 8. LC and SC have opposite effects on immunotherapy. Cartoon illustration of the concept of optimizing chemotherapy in the setting of immunotherapy: SC shows an indiscriminate toxicity toward cancer cells and the immune system, whereas LC enhances immunotherapy by destroying the tumor microenvironment and attracting activated immune cells toward the tumor area.

ulation resulting from chemotherapy-induced tumor cell death at the first week of polymer implantation continues to attract effector T cells into the tumor; the decreased concentration of BCNU on the second week after polymer implantation allows for effector T cells to exert their antitumor function. Both LC and SC increased the percentage of T_{reg} cells at days 21 and 30. The addition of anti–PD-1 to LC (unlike SC) decreased the percentage of T_{reg} cells at days 21 and 30, resulting in an increased T_{eff}/T_{reg} ratio in the LC + anti–PD-1 group at day 30. As expected, the anti–PD-1 monotherapy group exhibited increased infiltration of TILs, with increased CD8+IFN-γ–producing cells and decreased CD4+FoxP3+ cells (16), whereas LC increased the CD4+FoxP3+ cells and provided an initial (day 21) moderate decrease of CD8+IFN-γ–producing cells. However, LC enriched the tumor microenvironment for CD8+IFN-γ–producing cells at day 30 compared to control.

The immune profile in the peripheral blood and lymphoid organs reflected the changes in the tumor microenvironment. SC depleted CD3+ cells in DLNs and peripheral blood and caused myelotoxicity. Although SC did not affect the percentage of CD8+IFN-γ–producing cells, it greatly depleted the number of cells present in the peripheral organs.

The rechallenge experiments show that anti–PD-1 therapy generates immunologic memory against tumor antigens, resulting in tumor rejection upon rechallenge. SC abrogated this effect. LC, however, allowed for persistent immunologic memory generated by anti–PD-1 therapy. Flow cytometric analysis of rechallenged mice supports the hypothesis that SC disrupts memory T cell function. Analysis of TEM cells from the peripheral lymphoid organs (DLNs, peripheral blood, and spleen) showed that cells from SC mice exhibit dysfunctional IFN-γ production compared to the anti–PD-1 or LC + anti–PD-1 groups. Furthermore, the lack of a complete antitumor response in mice rechallenged with SC + anti–PD-1 after adoptive transfer of CD8 cells from LC + anti–PD-1 mice that rejected the tumor upon rechallenge implies that CD8 memory cells alone are not sufficient to produce a rapid and complete antitumor response. By putting the results of the survival data and the rechallenge-memory response together, we postulate that the late recurrence after SC could be attributed to two factors: (i) acquired mutations of the tumor after use of DNA-damaging agents and (ii) the lack of effector memory cells that can eliminate tumor clones encountered in the past but not successfully eliminated at that time. Additionally, SC + postrechallenge anti–PD-1 mice did not show survival or immunologic response to

utility of combining chemotherapy and immunotherapy. Mice treated with LC + anti–PD-1 showed a decreased number of CD4+FoxP3+ cells and an increase in CD8+IFN-γ–producing cells compared to mice in monotherapy or control groups. Immune infiltration of CD8+IFN-γ–producing cells was seen at day 30, but not day 21, which could indicate the local cytoreductive effect of BCNU giving way to immune activation. The interaction between LC and anti–PD-1 treatment and its effect on immune infiltration likely occur on two fronts: the cytoreductive effect of BCNU is concentrated within the first week after polymer implantation (days 14 to 21 after implantation) because of the kinetics of BCNU release from polymer (10). The presence of BCNU in the tumor microenvironment causes cell death and decreased proliferation of immune cells infiltrating the microenvironment at day 21, as seen with other chemotherapeutic agents (11, 15). Persistent antigen stim-

anti–PD-1 treatment as we would expect in chemotherapy-naïve anti–PD-1–treated mice. Our results suggest the need to optimize chemotherapy strategies for the treatment of newly diagnosed and recurrent GBM.

The current standard of care includes chemotherapy and radiation for newly diagnosed and recurrent GBM. Our results suggest that locally delivered chemotherapy can enhance the effects of immunotherapy. We therefore propose that the current approach to chemotherapy should be reassessed. Rather than viewing chemotherapy as a definitive therapy, we should consider chemotherapy as an initiator of a definitive immune-based therapy. Because BCNU-eluting polymers are currently approved for use in recurrent and newly diagnosed GBM, this strategy may be readily translated into clinical trials. We have also demonstrated that the timing of chemotherapy can affect the efficacy of immunotherapy. Currently, immunotherapy is typically administered after patients have failed their initial chemotherapy regimen. Our data suggest that administering SC before immunotherapy could inhibit the ability of the immune system to generate an effective antitumor immune response. This study suggests alternative therapeutic strategies to circumvent the negative immunologic profile of chemotherapy and optimize the combination of chemotherapy and immunotherapy for GBM.

MATERIALS AND METHODS

Study design
The objective of this study was to evaluate the optimal conditions under which chemotherapy and immunotherapy can synergize for the treatment of GBM. BCNU as well as TMZ were used as chemotherapy drugs of choice, either in the form of LC or SC at varying doses. Anti–PD-1 mAb was used as the immunotherapy of interest. Anti–PD-1 was used either before or after chemotherapy. Mice from varying treatment groups were followed to create survival curves, imaged to assess tumor progression, and rechallenged with tumor to assess immune memory. Mice were euthanized to assess the phenotype of the peripheral immune system as well as the tumor microenvironment at various time points. Although no power analysis was performed before the initiation of the experiments, we used a standard number of mice based on our previous experience with immune checkpoint inhibitors. Mice were randomized to different treatment groups on the basis of bioluminescent imaging to make sure that all treatment groups were starting with similar tumor sizes. The studies reported here were not blinded. All experiments were run in triplicates, except if specified otherwise.

Tumor model
Female C57BL/6J mice, 6 to 8 weeks old, were implanted (day 0) with GL261 LUC cells to establish intracranial gliomas, as previously described (16). Briefly, mice were anesthetized with ketamine (100 mg/kg)/xylazine (10 mg/kg), and a small midline incision was made to expose the skull. A burr hole was drilled directly over the striatum, and 130,000 GL261 LUC cells were implanted at a depth of 3 mm from the cortical surface. The tumor take rate was 100%. On day 7 after implantation, mice were imaged to assess tumor growth using an IVIS platform (In Vivo Imaging System, Caliper Life Sciences). Mice were stratified into experimental treatment groups based on luminescence. Each treatment group had 5 to 15 mice in survival experiments. The treatment groups were as follows: control [3% ethanol in phosphate-buffered saline (PBS), administered intraperitoneally], EP, anti–PD-1, LC, SC (3% ethanol in PBS), SC + anti–PD-1, and LC + anti–PD-1. All experiments were repeated at least three times unless otherwise stated.

For the SC groups, intraperitoneal BCNU was used in the following doses: 5, 15, and 30 mg/kg. TMZ was used in the following dose: 66 mg/kg daily from days 10 to 14. Anti–PD-1 was administered intraperitoneally at a dose of 200 μg on days 10, 12, and 14. Mice were euthanized at humane end points (severe neurological deficit that does not permit the mice to feed themselves, head tilt, or cachexia), as designated by our Institutional Animal Care and Use Committee.

Drugs
BCNU and TMZ were purchased from Sigma-Aldrich and dissolved in 100% ethanol in preparation for the intraperitoneal injection. The doses used were equivalent to human clinical doses. For more details on preparation, see the Supplementary Materials and Methods.

Surgical procedure: Polymer implantation
Mice in the LC or EP treatment groups were anesthetized with ketamine (100 mg/kg)/xylazine (10 mg/kg). The skin was prepared with alcohol swabs, a midline skin incision was opened, and the burr hole created for tumor implantation was identified. The burr hole was redrilled to allow for the polymer to enter the cranial cavity. The tumor mass was identified, and the polymer was placed directly on top of the tumor and pushed under the skull. The skin incision was closed with staples. Mice were monitored for a period of 30 min after recovery from anesthesia for signs of neurological deficits.

Anti–PD-1 mAb
Hamster anti-murine PD-1 mAb–producing hybridoma (G4) was used to produce antibody as previously described (17). Hamster immunoglobulin isotype (Rockland Immunochemicals Inc.) antibody was administered to animals receiving either BCNU polymers alone or intraperitoneal BCNU alone.

Statistics
Survival was plotted using Kaplan-Meier curves and analyzed with the log-rank Mantel-Cox test in GraphPad Prism software. For comparison of cell numbers and percentages between treatment groups in flow cytometry experiments, a two-tailed unpaired t test was used. P values <0.05 were considered significant. Figure 2 (B and E) was created after combining two separate experiments with similar survival to assume enough power to detect statistically significant values.

SUPPLEMENTARY MATERIALS
www.sciencetranslationalmedicine.org/cgi/content/full/8/370/370ra180/DC1
Materials and Methods
Fig. S1. Effects of LC, SC, and anti–PD-1 on BM myeloid cell subpopulations.
Fig. S2. Progression of intracranially implanted GL261 tumors for all treatment groups measured by bioluminescent imaging.
Fig. S3. Lymphopenia in the DLNs and PBLs after treatment with SC.
Fig. S4. Flow cytometric analysis of tumor-infiltrating immune cells in mice receiving chemotherapy, anti–PD-1, or combination therapy.
Fig. S5. Effect of adoptive transfer of CD8+ cells from LC + anti–PD-1 R to SC + anti–PD-1 R mice on tumor growth.
Fig. S6. Gating strategy of flow cytometric analysis of peripheral lymphocytes and TILs.
References (18–21)

REFERENCES AND NOTES
1. R. Stupp, M. E. Hegi, W. P. Mason, M. J. van den Bent, M. J. B. Taphoorn, R. C. Janzer, S. K. Ludwin, A. Allgeier, B. Fisher, K. Belanger, P. Hau, A. A. Brandes, J. Gijtenbeek, C. Marosi, C. J. Vecht, K. Mokhtari, P. Wesseling, S. Villa, E. Eisenhauer, T. Gorlia, M. Weller, D. Lacombe, J. G. Cairncross, R.-O. Mirimanoff; European Organisation for Research and

Treatment of Cancer Brain Tumour and Radiation Oncology Groups, National Cancer Institute of Canada Clinical Trials Group, Effects of radiotherapy with concomitant and adjuvant temozolomide versus radiotherapy alone on survival in glioblastoma in a randomised phase III study: 5-Year analysis of the EORTC-NCIC trial. *Lancet Oncol.* **10**, 459–466 (2009).

2. W. H. Brooks, M. G. Netsky, D. E. Normansell, D. A. Horwitz, Depressed cell-mediated immunity in patients with primary intracranial tumors. Characterization of a humoral immunosuppressive factor. *J. Exp. Med.* **136**, 1631–1647 (1972).

3. S. A. Grossman, X. Ye, G. Lesser, A. Sloan, H. Carraway, S. Desideri, S. Piantadosi; NABTT CNS Consortium, Immunosuppression in patients with high-grade gliomas treated with radiation and temozolomide. *Clin. Cancer Res.* **17**, 5473–5480 (2011).

4. G. Lombardi, E. Rumiato, R. Bertorelle, D. Saggioro, P. Farina, A. Della Puppa, F. Zustovich, F. Berti, V. Sacchetto, R. Marcato, A. Amadori, V. Zagonel, Clinical and genetic factors associated with severe hematological toxicity in glioblastoma patients during radiation plus temozolomide treatment: A prospective study. *Am. J. Clin. Oncol.* **38**, 514–519 (2013).

5. J. R. Brahmer, H. Hammers, E. J. Lipson, Nivolumab: Targeting PD-1 to bolster antitumor immunity. *Future Oncol.* **11**, 1307–1326 (2015).

6. S. L. Topalian, F. S. Hodi, J. R. Brahmer, S. N. Gettinger, D. C. Smith, D. F. McDermott, J. D. Powderly, R. D. Carvajal, J. A. Sosman, M. B. Atkins, P. D. Leming, D. R. Spigel, S. J. Antonia, L. Horn, C. G. Drake, D. M. Pardoll, L. Chen, W. H. Sharfman, R. A. Anders, J. M. Taube, T. L. McMiller, H. Xu, A. J. Korman, M. Jure-Kunkel, S. Agrawal, D. McDonald, G. D. Kollia, A. Gupta, J. M. Wigginton, M. Sznol, Safety, activity, and immune correlates of anti–PD-1 antibody in cancer. *N. Engl. J. Med.* **366**, 2443–2454 (2012).

7. D. M. Pardoll, The blockade of immune checkpoints in cancer immunotherapy. *Nat. Rev. Cancer* **12**, 252–264 (2012).

8. R. G. van der Most, B. W. Robinson, R. A. Lake, Combining immunotherapy with chemotherapy to treat cancer. *Discov. Med.* **5**, 265–270 (2005).

9. C. Jackson, J. Ruzevick, H. Brem, M. Lim, Vaccine strategies for glioblastoma: Progress and future directions. *Immunotherapy* **5**, 155–167 (2013).

10. A. B. Fleming, W. M. Saltzman, Pharmacokinetics of the carmustine implant. *Clin. Pharmacokinet.* **41**, 403–419 (2002).

11. A. J. Litterman, A. Z. Dudek, D. A. Largaespada, Alkylating chemotherapy may exert a uniquely deleterious effect upon neoantigen-targeting anticancer vaccination. *Oncoimmunology* **2**, e26294 (2013).

12. D. T. Le, E. M. Jaffee, Regulatory T-cell modulation using cyclophosphamide in vaccine approaches: A current perspective. *Cancer Res.* **72**, 3439–3444 (2012).

13. Y. Hailemichael, W. W. Overwijk, Cancer vaccines: Trafficking of tumor-specific T cells to tumor after therapeutic vaccination. *Int. J. Biochem. Cell Biol.* **53**, 46–50 (2014).

14. O. Preynat-Seauve, P. Schuler, E. Contassot, F. Beermann, B. Huard, L. E. French, Tumor-infiltrating dendritic cells are potent antigen-presenting cells able to activate T cells and mediate tumor rejection. *J. Immunol.* **176**, 61–67 (2006).

15. A. J. Litterman, D. M. Zellmer, K. L. Grinnen, M. A. Hunt, A. Z. Dudek, A. M. Salazar, J. R. Ohlfest, Profound impairment of adaptive immune responses by alkylating chemotherapy. *J. Immunol.* **190**, 6259–6268 (2013).

16. J. Zeng, A. P. See, J. Phallen, C. M. Jackson, Z. Belcaid, J. Ruzevick, N. Durham, C. Meyer, T. J. Harris, E. Albesiano, G. Pradilla, E. Ford, J. Wong, H.-J. Hammers, D. Mathios, B. Tyler, H. Brem, P. T. Tran, D. Pardoll, C. G. Drake, M. Lim, Anti-PD-1 blockade and stereotactic radiation produce long-term survival in mice with intracranial gliomas. *Int. J. Radiat. Oncol. Biol. Phys.* **86**, 343–349 (2013).

17. F. Hirano, K. Kaneko, H. Tamura, H. Dong, S. Wang, M. Ichikawa, C. Rietz, D. B. Flies, J. S. Lau, G. Zhu, K. Tamada, L. Chen, Blockade of B7-H1 and PD-1 by monoclonal antibodies potentiates cancer therapeutic immunity. *Cancer Res.* **65**, 1089–1096 (2005).

18. J. R. Ohlfest, B. M. Andersen, A. J. Litterman, J. Xia, C. A. Pennell, L. E. Swier, A. M. Salazar, M. R. Olin, Vaccine injection site matters: Qualitative and quantitative defects in CD8 T cells primed as a function of proximity to the tumor in a murine glioma model. *J. Immunol.* **190**, 613–620 (2013).

19. T. Reithmeier, E. Graf, T. Piroth, M. Trippel, M. O. Pinsker, G. Nikkhah, BCNU for recurrent glioblastoma multiforme: Efficacy, toxicity and prognostic factors. *BMC Cancer* **10**, 30 (2010).

20. R. J. Tamargo, J. S. Myseros, J. I. Epstein, M. B. Yang, M. Chasin, H. Brem, Interstitial chemotherapy of the 9L gliosarcoma: Controlled release polymers for drug delivery in the brain. *Cancer Res.* **53**, 329–333 (1993).

21. M. L. Affronti, C. R. Heery, J. E. Herndon II, J. N. Rich, D. A. Reardon, A. Desjardins, J. J. Vredenburgh, A. H. Friedman, D. D. Bigner, H. S. Friedman, Overall survival of newly diagnosed glioblastoma patients receiving carmustine wafers followed by radiation and concurrent temozolomide plus rotational multiagent chemotherapy. *Cancer* **115**, 3501–3511 (2009).

Mathios *et al.*, *Sci. Transl. Med.* **8**, 370ra180 (2016)   21 December 2016

12 of 12

Science Translational Medicine

Anti−PD-1 antitumor immunity is enhanced by local and abrogated by systemic chemotherapy in GBM

Dimitrios Mathios, Jennifer E. Kim, Antonella Mangraviti, Jillian Phallen, Chul-Kee Park, Christopher M. Jackson, Tomas Garzon-Muvdi, Eileen Kim, Debebe Theodros, Magdalena Polanczyk, Allison M. Martin, Ian Suk, Xiaobu Ye, Betty Tyler, Chetan Bettegowda, Henry Brem, Drew M. Pardoll and Michael Lim

Combining drugs as the doctor ordered

Cancer immunotherapy is rapidly increasing in prominence and being applied for a growing number of cancer types. Chemotherapy is still the mainstay of cancer treatment, however, and it can be difficult to find good ways to combine the two approaches. Mathios *et al.* addressed this problem by systematically evaluating the effectiveness of local or systemic chemotherapy given before or after immune checkpoint inhibition in mouse models of glioblastoma. The authors demonstrated that local chemotherapy was particularly effective in combination with checkpoint inhibition, whereas systemic chemotherapy was too damaging to the immune system to make for useful combinations.

ARTICLE TOOLS	http://stm.sciencemag.org/content/8/370/370ra180
SUPPLEMENTARY MATERIALS	http://stm.sciencemag.org/content/suppl/2016/12/19/8.370.370ra180.DC1
RELATED CONTENT	http://stm.sciencemag.org/content/scitransmed/8/328/328rv4.full http://stm.sciencemag.org/content/scitransmed/7/315/315ra188.full http://stm.sciencemag.org/content/scitransmed/7/283/283ra52.full http://stm.sciencemag.org/content/scitransmed/7/280/280sr1.full http://stm.sciencemag.org/content/scitransmed/9/389/eaal3604.full http://stm.sciencemag.org/content/scitransmed/9/393/eaal4922.full http://stm.sciencemag.org/content/scitransmed/9/399/eaaa0984.full
REFERENCES	This article cites 21 articles, 8 of which you can access for free http://stm.sciencemag.org/content/8/370/370ra180#BIBL
PERMISSIONS	http://www.sciencemag.org/help/reprints-and-permissions

Use of this article is subject to the Terms of Service